Non-perfect Channel Estimation in OFDM-MIMO-based Underwater Communication

Knut Grythe, Jan Erik Håkegård
SINTEF ICT, N-7465 Trondheim,
Norway

***Abstract*- The main focus in this publication is on the mean square error of underwater acoustic channel estimators as function of the delay and Doppler spreads of the channel, and the effect this estimation error has on the bit error rate performance of the system both using conventional single antennas (SISO) and when using multiple antennas (MIMO). It is investigated at which delay and Doppler spreads the decoding of the signal in the receiver becomes erroneous. It is assumed that there is no non-uniform Doppler shift. The radio communication standard IEEE 802.16e is modified to match underwater communication conditions. The system parameters are taken from measurements conducted in the Trondheim harbour in Norway in 2007. The channel estimator used is not optimal in the Wiener interpolator sense. Hence, the estimator is sub-optimal, but shows good performance and has relatively low complexity. For the described communication system to perform well the results indicate that movements in the water should be less than 0.01-0.1 m/s, and delay spreads should be less than 0.05-0.5 ms. In systems where the main problem is large Doppler spread, the number of sub-carriers should be small. In systems where the main problem is large delay spread, the number of sub-carriers should be large. The use of MIMO makes the system more robust against estimation errors. The density of pilot symbols may be increased to reduce the channel estimation error somewhat, at the expense of reduced efficiency. Considering the Trondheim harbour channel measurement results and their variability throughout the year, we find that the tested system copes well with the summer conditions while the winter conditions seems to be more challenging.**

I. INTRODUCTION

The authors are involved in the development of an underwater sensor network that may be used for e.g. environmental and biomass monitoring in the coastal- and ocean areas of Norway, including arctic regions. The main communication solution between the sensor nodes will be based on acoustic links. An illustration of the network deployment topology is given in Figure 1.

Traditionally, underwater acoustic communication systems have been based on non-coherent detection techniques such as Frequency Shift Keying (FSK) characterized by high reliability rather than bandwidth efficiency. However, during the last years a number of scientific publications have assessed coherent solutions for underwater communications, and measurements and trials have been conducted. In particular solutions based on OFDM have generated significant interest due to OFDM's good complexity-performance trade-off for frequency dispersive channels.

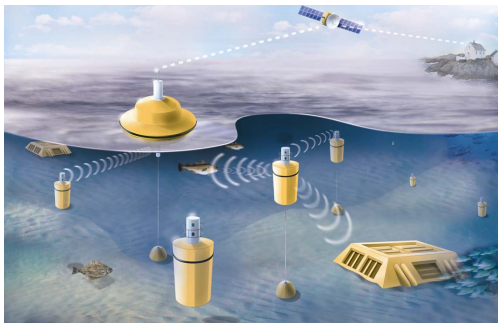

Figure 1. Illustration of topology and deployment of an underwater sensor network

There are two important challenges related to underwater OFDM communications. The first one is non-uniform Doppler shift across the sub-carriers. In traditional radio communications, the center frequency is so high compared to the signal bandwidth that the Doppler shift resulting from movements of the transmitter or receiver can be considered constant for all sub-carriers. This is not the case for underwater communications, leading to loss of orthogonality between sub-carriers and hence introducing Inter Channel Interference (ICI). Algorithms for non-uniform Doppler compensation are proposed in e.g. [1]. The second challenge is the double spread fading channel, possessing both long delay spreads in the order of milliseconds of even tens of milliseconds and Doppler spreads in the order of several Hertz, making accurate channel estimation and coherent detection difficult. The main remedies for these channel impairments are powerful codes such as LDPC codes and MIMO techniques (see e.g. [2]), allowing the receiver to yield good performance at low signal-to-noise ratios (SNRs). Most experimental results found in the literature are however obtained with relatively favorable channel conditions with delay spreads in the order of a few milliseconds and small Doppler spreads. Other strategies have been proposed for severely dispersive channels, such as passive time reversal for impulse response shortening [3]. A coherent alternative to multi-carrier communication is traditional single carrier communication, involving high complexity equalization in the receiver. To reduce the complexity, channel shortening and

solutions based on sparse channel impulse response assumption have been proposed (see e.g. [4]).

As a part of the communication tradeoff work, acoustic channel measurement campaigns were carried out in 2007 in shallow waters at the harbour of Trondheim. The measurements encompass both single input single output SISO and 2x2 multiple input multiple output MIMO transducer constellations. The purpose was to obtain additional experimental channel parameters from local areas.

The remaining of this paper is organised as follows. Section II presents the measurement site in the Trondheim harbour. Measurement results and channel analyses and properties like observed delay spread and Doppler spread are given in Section III. In Section IV the system under consideration is described, including the relevant parts of the IEEE802.16 standard and the adaptations that are made to it. In Section V, a comparison is made between the propagation conditions for radio communication in air and for acoustic communication in water. In Section VI, simulation results of the performance are given before conclusions are finally drawn in Section VII.

II. MEASUREMENT SITE

Figure 2 shows an overview of the link. The sea depth profile along the transmission path is shown in Figure 3. The bottom is mainly sand and silt, with low to moderate reflectivity. Sound propagation properties of the link depend heavily on the sound speed profile vs. depth. A non-uniform sound speed will bend rays up or down, influencing the channel impulse response very much. The conditions, especially close to the water surface, showed large diurnal and seasonal variation. In addition to temperature, a combination of tide and fresh water from a nearby river is important. This is typical for harbours and coastal areas.

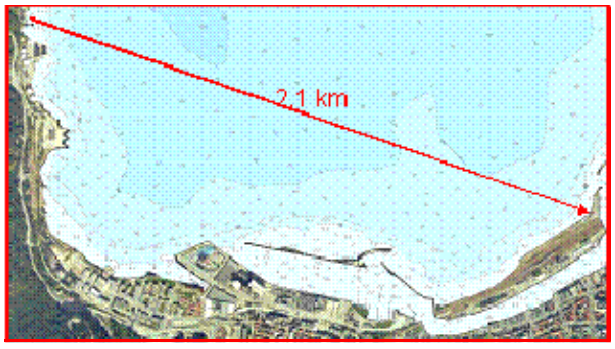

Figure 2. Trondheim harbour link layout

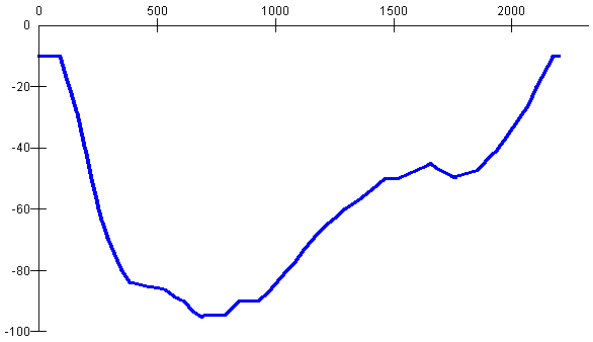

Figure 3. Water depth profile. Transmission direction was from left to right.

Sound speed profiles were measured using a standard CTD instrument, once for each measurement day. Figure 4 shows three examples. All cases show more or less tendency to a surface duct (rays bending upwards close to the surface).

Transducers were lowered into the water from piers at each side of the link, resulting in stable transducer positions. Rapid channel variations (Doppler) are therefore mainly due to sea surface waves. The distance from the top of the upper transducer to the water surface varied between 1.3 and 2.7 meters when measuring.

To carry out Single Input Single Input (SISO) and 2x2 Multiple Input Multiple Output (MIMO) measurements, four identical transducers were used, two at each end of the link. The centre frequency was 38 kHz with a bandwidth of about 4 kHz. In the MIMO case, the two transducers at each side were positioned vertically, about 8 wavelengths apart

The transmitted signals were BPSK modulated Kasami sequences of lengths 127 and 255 bits and with symbol rate equal to 3 ksps. Each transducer transmitted a different Kasami sequence.

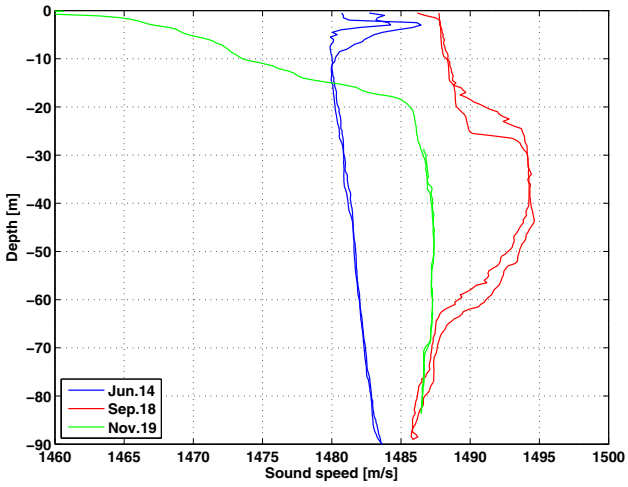

Figure 4. Sound speed profiles (double curves are down and up direction CTD measurements).

The transmitter symbol shaping was done with a roll-off factor of 0.5. Sequences were stacked head to tail into measurement runs of about 60 - 70 seconds durations. This resulted in roughly 1500 or 750 consecutive received PN sequences respectively.

III. MEASUREMENT RESULTS

A. Channel characterization

Like the well known wireless channel, the underwater channel is time-varying. This means that the input-output relationship between a transmitted signal $x(t)$ and the received signal $y(t)$ can be written like

$$y(t) = \int h(t-\tau,\tau)x(t-\tau)d\tau \tag{1}$$

The kernel of this integral operator is sometimes referred to as the time-varying impulse response or the (Output) Delay-Spread function, and is usually modeled as the realization of a stochastic process.

Since $h(t,\tau)$ is a random variable the characterization of the channel is a question of estimating its statistics. The second order statistics of the channel is expressed in the form of the autocorrelation function

$$A(t,t',\tau,\tau') = E\left[h(t,\tau)h^*(t',\tau')\right]. \tag{2}$$

It is clearly unpractical to work with this function, which in turn forces us to make some simplifying assumptions about the channel.

The first assumption is that the channel is wide sense stationary (WSS), that is, the first and second moments of the channels do not depend on the time t. The second assumption is that the reflected signals from different scatters are uncorrelated (US). Combining these two assumptions gives us a WSSUS channel [5], which in turn can be written as

$$\begin{aligned} A(t,t',\tau,\tau') &= E\left[h(t,\tau)h^*(t',\tau')\right]\delta(\tau-\tau') \\ &= E\left[h(0,\tau)h^*(t'-t,\tau')\right]\delta(\tau-\tau') \\ &= Q(\xi,\tau) \end{aligned} \tag{3}$$

This function is referred to as the Delay Cross-Power Spectral Density. An immediate function that is obtained from $Q(\xi,\tau)$ is the Delay Power Density Spectrum, $Q(\tau)=Q(0,\tau)$. This function enables us to calculate the root mean square (rms) delay spread of the channel,

$$\mu_\tau = \frac{\int \tau Q(\tau)d\tau}{\int Q(\tau)d\tau}, \sigma_\tau = \sqrt{\frac{\int(\tau-\mu_\tau)^2 Q(\tau)d\tau}{\int Q(\tau)d\tau}} \tag{4}$$

$Q(\xi,\tau)$ is also the basis for a set of descriptive functions that are obtained by calculating the Fourier transform of $Q(\xi,\tau)$ with respect to one or both variables. We are in particular interested in the Doppler Cross-Power Spectral Density, $P(f,\omega)$, which is obtained by Fourier transforming $Q(\xi,\tau)$ with respect to both variables. From this we can obtain the Doppler Power Density Spectrum, $P(f)= P(f,0)$. From this function we obtain another important channel parameter, the rms Doppler spread

$$\mu_f = \frac{\int fP(f)df}{\int P(f)df}, \sigma_f = \sqrt{\frac{\int(f-\mu_f)^2 P(f)df}{\int P(f)df}} \tag{5}$$

The rms delay and Doppler spreads are the two single most important parameters that characterize the channel, as they indicate how much memory the channel has, and how quickly the channel changes.

B. Measurement results

The Delay Power Density Spectrum, $Q(\tau)=Q(0,\tau)$ is illustrated in Figure 5. Care must be taken when calculating the rms Delay spread however, as the existence of a noise floor will make the estimate arbitrarily large as the domain of integration is extended. The solution is to threshold the Delay Power Density Spectrum to some robust value above the noise floor and in that way exclude the noise. For our experiments the threshold was set heuristically to -6dB relative to the maximum of the Delay Power Density Spectrum after visual inspection. Finally, a qualitative glance at Figure 5 tells us that the channel has a length of roughly 2 ms, which in turn means that the memory is 6 symbols for a symbol rate of 3 kHz.

To obtain the Doppler Power Spectrum Density we first need to calculate the Doppler Cross-Power Spectral Density, $P(f,\omega)$, which in the discrete case is the 2D-FFT of $Q(\xi,\tau)$. Setting $\omega=0$ yields the Doppler Power Spectrum Density, $P(f)$. The resulting function is plotted in Figure 6. To visualise the influence of the velocity profiles shown in Figure 4, we show in Figure 7 to Figure 9 examples of the magnitude of the corresponding impulse responses in the delay-time domain.

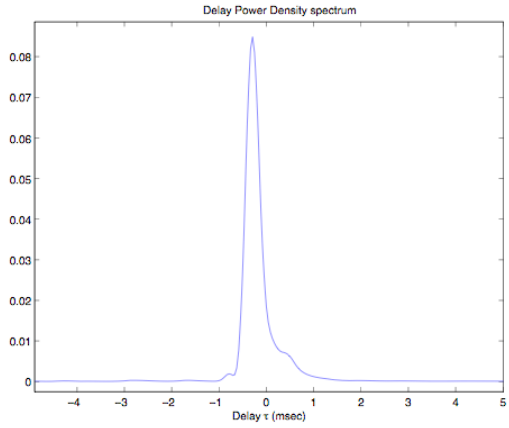

Figure 5. Delay Power Density Spectrum, $Q(\tau)=Q(0,\tau)$. (June 2007).

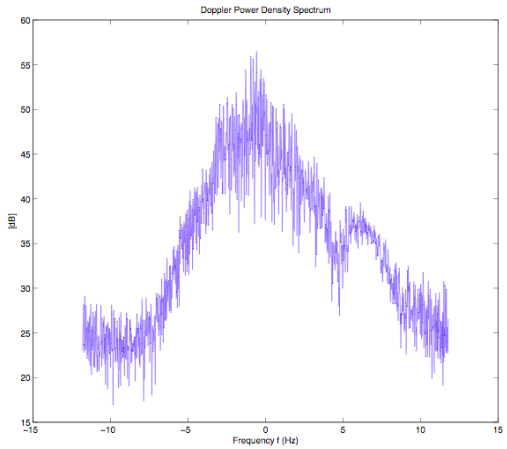

Figure 6 Doppler Spectral Density, *P(f)=P(f,0)*. (June 2007).

The November responses can be observed to be very blurred in the delay domain compared to June and September. Some results for the rms Delay spread and rms Doppler spread for the June, September and November campaigns are given in TABLES 1, 2 and 3.

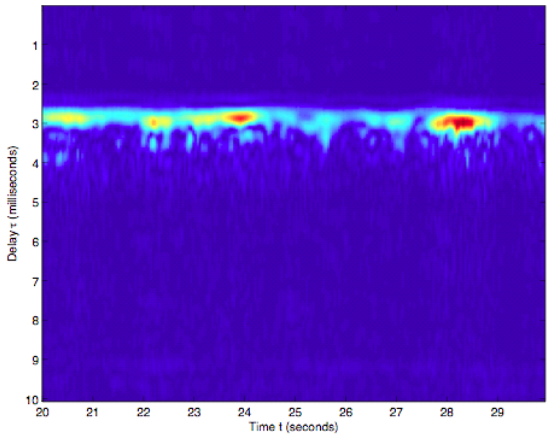

Figure 7. June, magnitude impulse response example.

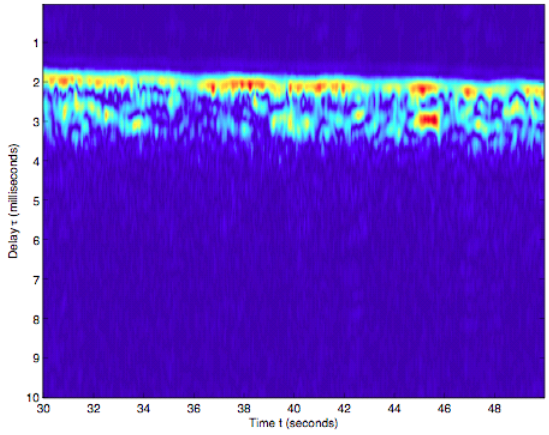

Figure 8. September, magnitude impulse response example.

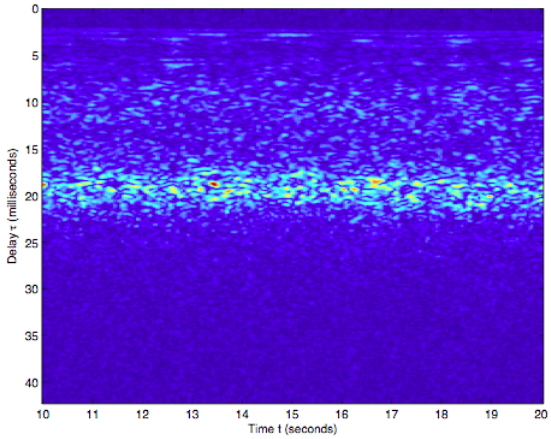

Figure 9. November, magnitude impulse response example.

TABLE 1
MEASUREMENT EXAMPLES FOR JUNE 2007

RMS Delay spread (Sec)	RMS Doppler spread (Hz)
1.6753e-04	1.8477
5.1702e-04	2.2286
3.5862e-04	2.5636
3.8006e-04	2.4434

TABLE 2
MEASUREMENT EXAMPLES FOR SEPTEMBER 2007

RMS Delay spread (Sec)	RMS Doppler spread (Hz)
3.4821e-04	1.2063
1.7817e-04	1.6635
7.6986e-04	0.8454
5.3052e-04	0.7680

TABLE 3
MEASUREMENT EXAMPLES FOR NOVEMBER 2007

RMS Delay spread (Sec)	RMS Doppler spread (Hz)
9.2650e-03	Not calculated
8.6275e-03	Not calculated

We find the Doppler spread to be in the order of 2 Hz in the June and around 1 Hz in September. The same Doppler range we expect to be true also for November since the wind conditions were almost identical. The average Delay spread is somewhat higher in September the June, 0.4 ms versus 0.24 ms. As can be observed from TABLE 3, the November channel has a larger Delay spread, in the order of 8 to 10 ms.

The theoretical communication capacities (SISO/MIMO) of the reported channels are presented in [6].

IV. Communication System Description

WiMAX systems are based on the IEEE802.16 standard. This work concentrates on the IEEE802.16e amendment of the standard developed for mobile users. The physical interface is based on OFDMA, which is a multiuser multicarrier modulation technique, in which the different sub-carriers of each symbol may be shared between several users. The bandwidth can be scaled from 1.25 MHz (corresponding to

128 sub-carriers) to 20 MHz (corresponding to 2048 sub-carriers), leading to significant flexibility in system design. The bandwidth of each sub-carrier is 10.94 kHz in all configurations leading to a constant OFDM symbol duration of 91.4 ms, not including the cyclic prefix.

Several coding and modulation schemes are contained in the standard. There are seven mandatory schemes including modulations from QPSK to 64 QAM and convolutional coding with rates 1/2, 2/3 and 3/4. The spectral efficiency can then be varied from one information bit per symbol to 4.5 information bits per symbol and hence enabling systems to adapt to varying received SNRs. In addition to the mandatory coding and modulation schemes there are several optional schemes based on iterative decoding (LDPC-codes and "turbo"-codes).

Multiple antenna techniques further enhance the performance of the technology. There are mainly two MIMO techniques included in the standard: Spatial Multiplexing (SM) and Space-Time Coding (STC). In spatial multiplexing, two transmit antennas transmit independent symbol streams, doubling the spectral efficiency with respect to conventional single antenna systems. In space-time coding, the Alamouti scheme is used to exploit transmit diversity and hence increase the BER performance at given channel conditions.

An important part of the receiver is the channel estimator, as coherent detection is required. Pilot symbols are embedded in the transmit signal in order to allow the receiver to track the channel variations due to multipath propagation. Several sub-carrier allocation schemes are included in the standard, and in this work we concentrate on DL-PUSC (Down Link Partial Usage of Sub-Carriers). The OFDM symbol is then divided into clusters of size 14x2, i.e. 14 sub-carriers and two symbols. For single antenna systems, each cluster contains 4 pilot symbols and 24 data symbols. The distribution of pilot symbols within a cluster for single antenna systems is illustrated in Figure 1. If the channel varies too fast, either across each symbol (i.e. in the frequency domain) or between symbols (i.e. in the time domain) the estimation error will be significant and jeopardize the decoding performance. In the simulator used in this work, a 2 dimensional cubic interpolator using Delaunay triangulation [8] is applied.

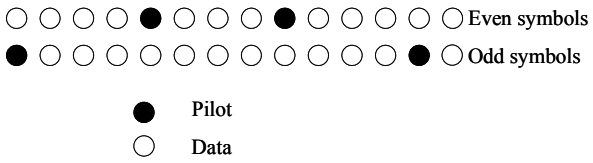

Figure 10 DL-PUSC cluster (SISO). Frequency in the horizontal direction.

V. COMPARISON BETWEEN RADIO AND UNDERWATER ACOUSTIC PROPAGATION

WiMAX systems may operate in many different frequency bands. However, they generally operate in licensed band such as the 2.3 GHz, 2.5 GHz or 3.5 GHz bands. As described earlier, the bandwidth may range from 1.25 MHz to 20 MHz. In order to compare WiMAX with underwater communications, the signal parameters are in this publication fixed to the values given in Table I.

Underwater communication systems may also operate at a range of frequencies and with different bandwidths. In the work previously presented, the parameters given in TABLE 4 were used.

Two important parameters determining the performance of the system is the Doppler spread f_d and the delay spread τ of the propagation channel. In order to compare the two systems the normalized versions of these parameters are convenient to use:

$$f_d^* = \frac{f_d}{\Delta f}, \tau^* = \frac{\tau}{T_s}, \quad (6)$$

where Δf is the sub-carrier bandwidth and T_s is the OFDM symbol length. These two system parameters are the inverse of each other: $\Delta f = 1/T_s$. A common way of classifying fading channels with respect to channel estimation is as follows. If $f_d{}^*$ (or similarly $\tau_d{}^*$) is:

- Smaller than 0.01: there is no problem to estimate the channel.
- Between 0.01 and 0.1: it is challenging to estimate the channel.
- Larger than 0.1: it is impossible to estimate the channel.

This classification can be used as guideline when assessing whether a system is able to communicate over a given channel.

TABLE 4 SIGNAL PARAMETERS

	Acoustic	Radio
Center frequency	38 kHz	2.5 GHz
Bandwidth	3 kHz	10 MHz
Propagation speed	1500 m/s	$3 \cdot 10^8$ m/s

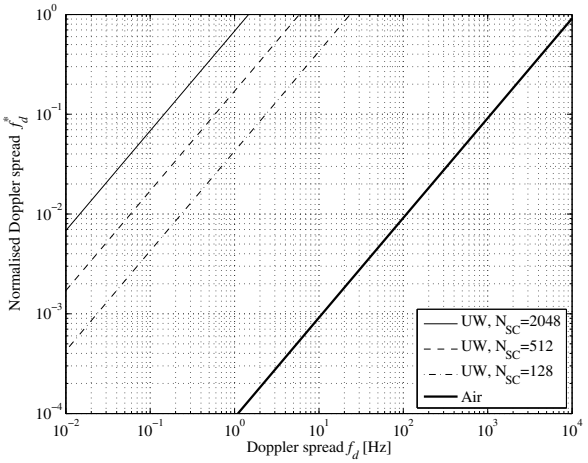

Figure 11 f_d^* for underwater communication

Figure 11 illustrates how the normalized Doppler spread corresponds to actual Doppler spread for communication systems in air and underwater. In order to make channel estimation straightforward, the maximum Doppler spread for a system in air will be about 100 Hz, while decoding may be possible up to 1 kHz. This corresponds to speeds of 12 m/s and 120 m/s, respectively, for a system operating at 2.5 GHz. Hence, in areas with a Rayleigh type of fading, decoding will become impossible for speeds somewhere between 43 km/h and 430 km/h, depending on the estimation techniques and other system aspects. Mobile WiMAX systems are designed to provide connection for vehicular speeds up to 120 km/h. For underwater communication, the total bandwidth is chosen to be fixed so that the bandwidth per sub-carrier depends on the number of sub-carriers N_{SC} . Figure 11 shows that the underwater communication system is much more sensitive to Doppler spread. For $N_{SC} = 128$, channel estimation errors make decoding impossible for $f_d > 2.5$ Hz corresponding to speeds above 0.1 m/s and straightforward for $f_d < 0.25$ Hz corresponding to speeds below 0.01 m/s. As the number of sub-carriers increases (and keeping the total bandwidth fixed to 3 kHz) the OFDM symbol length increases as well, making the system even more sensitive to Doppler spreads. For $N_{SC} = 2048$, channel estimation errors will make decoding impossible for speeds as low as 0.006 m/s.

In Fig 12, the relation between normalized delay spread and actual delay spread is illustrated. For the communication system in air, the delay spread should be less than 1 ms to avoid problems related to channel estimation. This corresponds to a difference in path length of 300 meters. Channel estimation errors make decoding troublesome for difference in path lengths in the order of 3 km. Underwater communication permits longer delay spread in time. A signal with 2048 sub-carriers may tolerate delay spreads as long as 7 ms without encountering problems with channel estimations and up to 70 ms before estimation errors make decoding very difficult. Fewer sub-carriers make each sub-carrier wider in frequency and hence the system more sensitive to channel estimation errors in the frequency domain. For $N_{SC} = 128$, channel estimation is straight forward for $\tau < 0.5$ ms, while estimation errors will make decoding very cumbersome for $\tau > 5$ ms. The delay spread actually encountered in a real system is very dependent on the environment and type of system as shown in Section III.

Designing a system for communication across a propagation channel exhibiting both delay and Doppler spreads will involve a compromise, as a large number of sub-carriers will provide a relatively good robustness against delay spread, but make the system more sensitive to Doppler spread. For channels experiencing varying conditions, the system should consequently be adaptive in terms of the number of sub-carriers used.

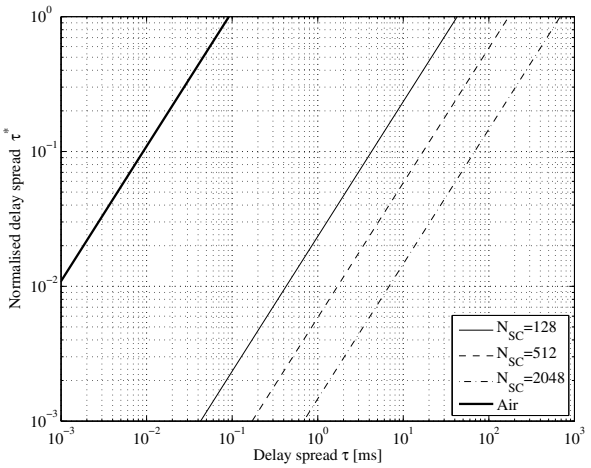

Figure 12 τ^* for underwater communication

VI. UNDERWATER SYSTEM PERFORMANCE

The results in the previous section are based on a very general rule. In order to verify that a WiMAX-like system adapted to underwater communication performs according to this rule, a simulator developed for WiMAX communication in air was adapted to underwater communications. The simulator includes all mandatory coding and modulation schemes and MIMO techniques included in the standard.

The channel model used in this work is a basic Rayleigh fading channel with additive white Gaussian noise, which is commonly used in analysis of radio communication systems. Most underwater acoustic channels have somewhat different characteristics than the traditional radio channel, and the modelling should reflect these differences. Moreover, the underwater propagation environment varies greatly, as equipment may be installed in rivers, in shallow water, in deep sea etc. To validate analytical and simulation results by real measurements is therefore even more important when assessing and developing underwater communication systems than for the more mature area of radio communications.

C. MSE performance of the channel estimator

In Figure 13 and Figure 14, the simulated MSE of the channel estimator as function of the Doppler spread is shown for 128 and 2048 sub-carriers, respectively. The curves show good correspondence with the results from the previous section. The curves corresponding to a normalized Doppler spread of 0.01 shows little degradation compared to the case of no Doppler spread, while the curves corresponding to a normalized Doppler spread of 0.1 exhibits an error floor that starts to appear at E_b / N_0 below 10 dB, which is lower than the operating point for most of the system configurations.

In Figure 15 and Figure 16 the simulated MSE as function of delay spread is illustrated without Doppler spread and with $N_{SC} = 128$ and $N_{SC} = 2048$, respectively. The channel is created using two taps of equal energy separated by τ , which is the worst case in the sense that the channel energy is spread

as far from the mean of the channel response as possible. The curves indicate that the general rule of the previous section also applies for delay spreads.

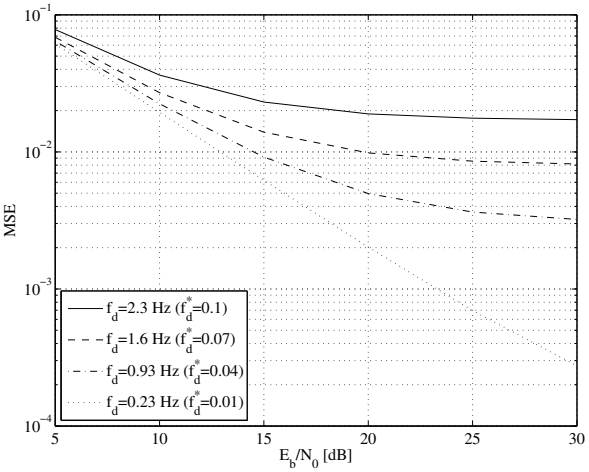

Figure 13 MSE of estimator with τ=0 ms, N_{sc}=128.

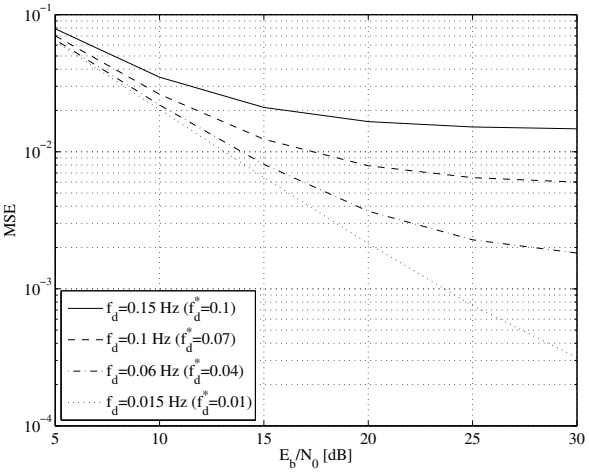

Figure 14 MSE of estimator with τ=0 ms, N_{sc}=2048.

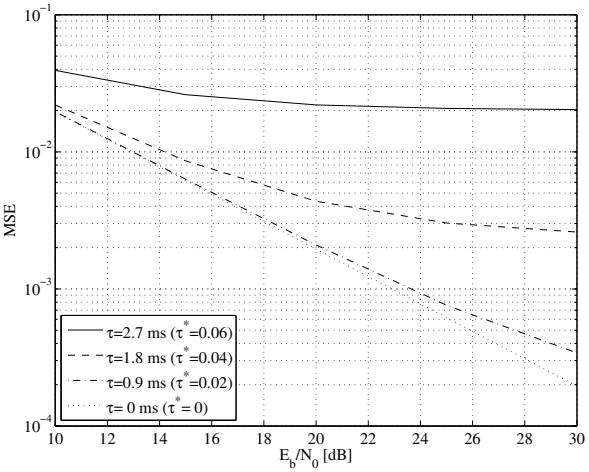

Figure 15 MSE of estimator for f_d=0 Hz, N_{sc}=128.

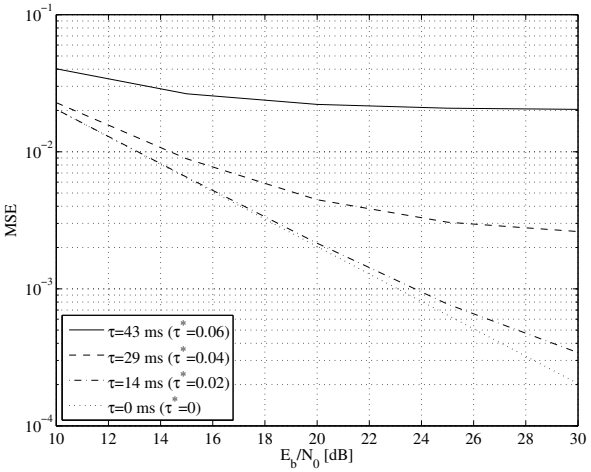

Figure 16 MSE of estimator for f_d=0 Hz, N_{sc}=2048.

D. BER performance of the system

Simulated BER with 1/2-rate convolutional coding, QPSK modulation and single transmit and receive antennas is shown in Figure 17 and Figure 18. The scheme corresponds to mode 1 coding in the IEEE802.16 standard. The curves indicate that the estimation error starts to become critical for Doppler spread around 1-2 Hz (corresponding to normalized Doppler spread around 0.05 and 0.1) and delay spread around 1 ms (corresponding to normalized delay spread in the order of 0.01). To obtain BERs in the order of 10-5, Doppler and delay spread should be lower than these figures.

In Figure 19 and Figure 20, the simulated BER is shown for 2x2 STC. The antenna elements both at the transmitter and receiver are assumed to be located so far from each other that the channels are uncorrelated and maximum diversity gain is obtained. The result is that the system may operate at lower SNRs than single antenna systems. As a result, the system becomes more robust against estimation errors as well.

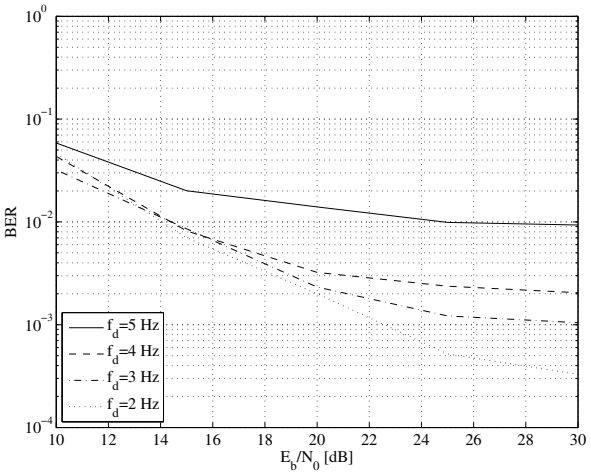

Figure 17 Simulated BER, SISO, rate-1/2 coding, QPSK, □=0 ms, Nsc=128.

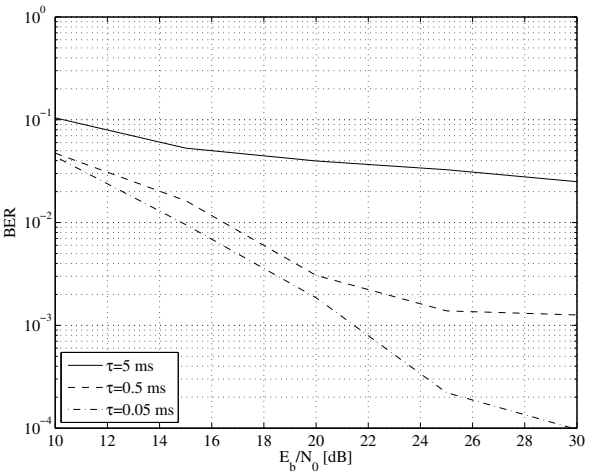

Figure 18 Simulated BER, SISO, rate-1/2 coding, QPSK, f_d=2 Hz, N_{sc}=128.

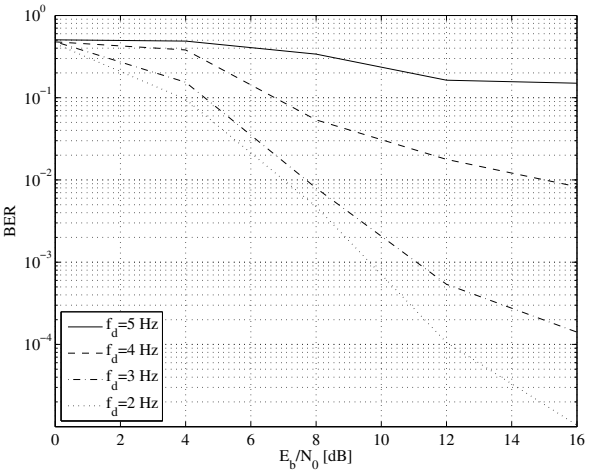

Figure 19 Simulated BER, STC, rate-1/2 coding, QPSK, τ=0 ms, N_{sc}=128.

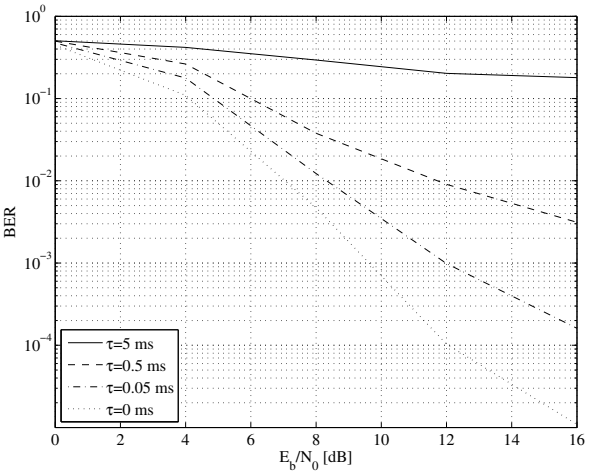

Figure 20 Simulated BER, STC, rate-1/2 coding, QPSK, fd=2 Hz, N_{sc}=128.

VII. CONCLUSIONS

This paper has presented measurements and derivative results from a 2007 underwater acoustical measurement campaign in the Trondheim harbour.

The acoustical velocity profile of the measurement link shows a high variability during the summer to November period, particularly in the upper 30 meters of the water column. This is influencing the propagation conditions and consequently when deploying underwater sensor networks in similar near coastal areas with river outlets, a propagation adaptive network topology should be sought for maximum connectivity and sensing reporting. The fixed structures used for the measurements resulted in very small Doppler spread of the signals.

The rather near-surface transducer installation probably made the upper velocity profiles to dominate the measured impulse responses. The delay spread shows relatively large variations during the period with a ratio of more than 20 between the maximum and minimum values. The maximum was observed in November with a value of around 8 - 10 ms.

Channel estimation in OFDM-based underwater communication is assessed together with the impact of estimation errors on system performance. The channel estimator used in this work is not optimal in the Wiener interpolator sense, which would require information about the statistical properties of the channel. The estimator used is sub-optimal, but shows good performance and has relatively low complexity. It therefore gives a good impression of the performance in real systems.

For the described system to perform well the results indicate that movements in the water should be less than 0.01-0.1 m/s, and delay spreads should be less than 0.05-0.5 ms. In systems where the main problem is large Doppler spread, the number of sub-carriers should be small. In systems where the main problem is large delay spread, the number of sub-carriers should be large. The use of MIMO makes the system more robust against estimation errors.

The density of pilot symbols may be increased to reduce the channel estimation error somewhat, at the expense of reduced efficiency. For severe delay spread in the order of tens of milliseconds channel shortening schemes may improve the performance. The effect of channel estimation errors may be reduced by using (in addition to MIMO techniques) more powerful codes such as LDPC codes.

ACKNOWLEDGMENT

This work was financed by the Norwegian Research Council project “Nordområdenes Nye Nervesystem, Undervanns Trådløst Sensornettverk” (Contract Number 176779).

We like to thank the NTNU Biological Institute and the Public Bath organisation of Trondheim for the permission to use their facilities during the measurements. Further the NTNU’s boat Gunnerus for performing the CTD measurements.

REFERENCES

[1]. B. Li *et al.,* "Multicarrier Communication over Underwater Acoustic Channels with Nonuniform Doppler Shifts," Proc. of MTS/IEEE OCEANS conference, Quebec, Canada, Sept. 15-18, 2008.

[2]. B. Li *et al.,* "Further Results on High-Rate MIMO-OFDM Underwater Acoustic Communications," Proc. of MTS/IEEE OCEANS conference, Quebec, Canada, Sept. 15-18, 2008.

[3]. J.. Gomes *et al.,* "OFDM Demodulation in Underwater Time-Reversed Shortened Channels," Proc. of MTS/IEEE OCEANS conference, Quebec, Canada, Sept. 15-18, 2008.

[4]. M. Stojanovic, "Efficient Processing of Acoustic Signals for High Rate Information Transmission over Sparse Underwater Channels," Elsevier Journal on Physical Communication, June 2008, pp.146-161.

[5]. Kilfoyle, D.B.; Baggeroer, A.B. "The state of the art in underwater acoustic telemetry". Oceanic Engineering, IEEE Journal of, Volume 25, Issue 1, Jan. 2000 Page(s):4 – 27.

[6]. K. Grythe *et al.*, "The Trondheim Harbour: Acoustic propagation measurements and communication capacity," Proc. of MTS/IEEE OCEANS conference, Quebec, Canada, Sept. 15-18, 2008.

[7]. J.E. Håkegård, K. Grythe, "Effects of Channel Estimation Errors in OFDM-MIMO-based Underwater Communications," Proc. of IEEE WUnderNet, May 27, 2009.

[8]. http://www.qhull.com